

Redox chemistry of Pt(II) complex with non-innocent NHC bis(phenolate) pincer ligand: electrochemical, spectroscopic and computational aspects

Ilya K. Mikhailov ^{1,2}, Zufar N. Gafurov ^{1,*}, Alexey A. Kagilev ^{1,2}, Vladimir I. Morozov ¹, Artyom O. Kantukov ^{1,2}, Ekaterina M. Zueva ^{1,3}, Gumar R. Ganeev ², Il'yas F. Sakhapov ¹, Asiya V. Toropchina ¹, Igor A. Litvinov ¹, Galina A. Gurina ⁴, Alexander A. Trifonov ^{4,5}, Oleg G. Sinyashin ¹, and Dmitry G. Yakhvarov ^{1,2,*}

¹ Arbuzov Institute of Organic and Physical Chemistry, FRC Kazan Scientific Center, Russian Academy of Sciences, Arbuzov Str. 8, Kazan, 420088, Russia; yakhvar@iopc.ru

² Kazan Federal University, Kremlovskaya Str. 18, Kazan, 420008, Russia

³ Department of Inorganic Chemistry, Kazan National Research Technological University, Karl Marx Str. 68, Kazan, 420015, Russia

⁴ Institute of Organometallic Chemistry of Russian Academy of Sciences, Tropinina str. 49, GSP-445, Nizhny Novgorod, 603950, Russia

⁵ A.N. Nesmeyanov Institute of Organoelement Compounds, Russian Academy of Sciences (INEOS RAS), Vavilova Str. 28, Moscow, 119991, Russia

* Correspondence: gafurov.zufar@iopc.ru (Z.N. Gafurov), yakhvar@iopc.ru (D.G. Yakhvarov).

Supplementary Materials

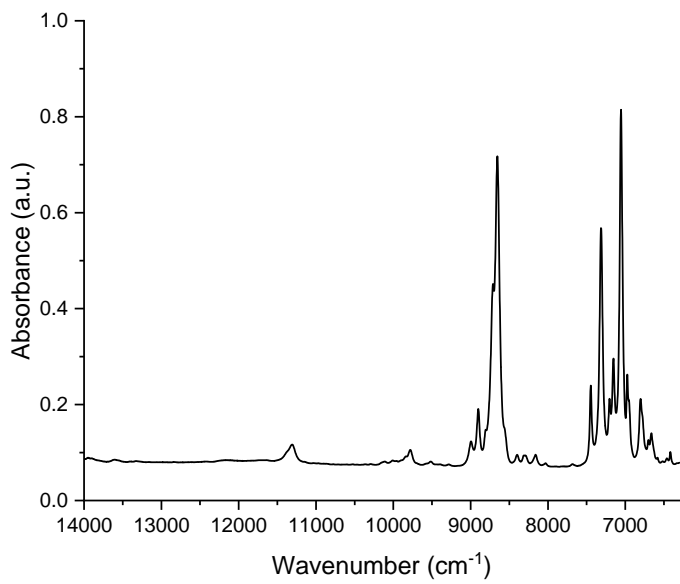


Figure S1. NIR spectrum of CH_2Cl_2 at 298 K, $l = 1 \text{ cm}$.

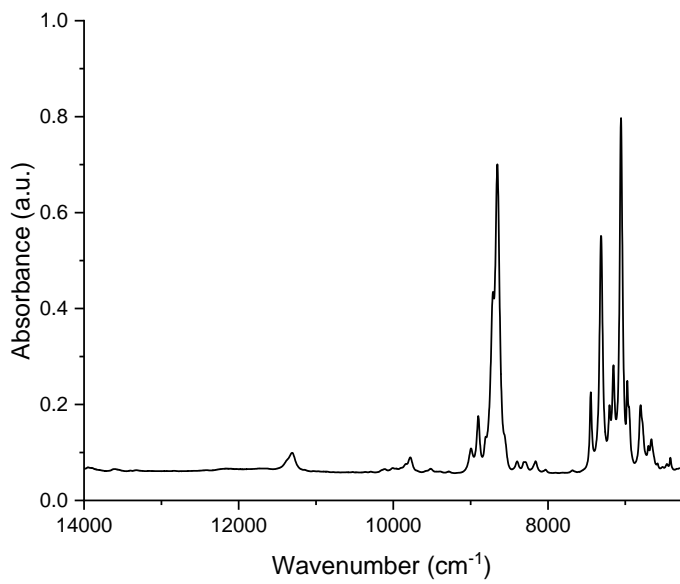


Figure S2. NIR spectrum of $\text{Pt}(\text{L})\text{Py}$ ($c = 0.1 \text{ mM}$) in CH_2Cl_2 at 298 K, $l = 1 \text{ cm}$.

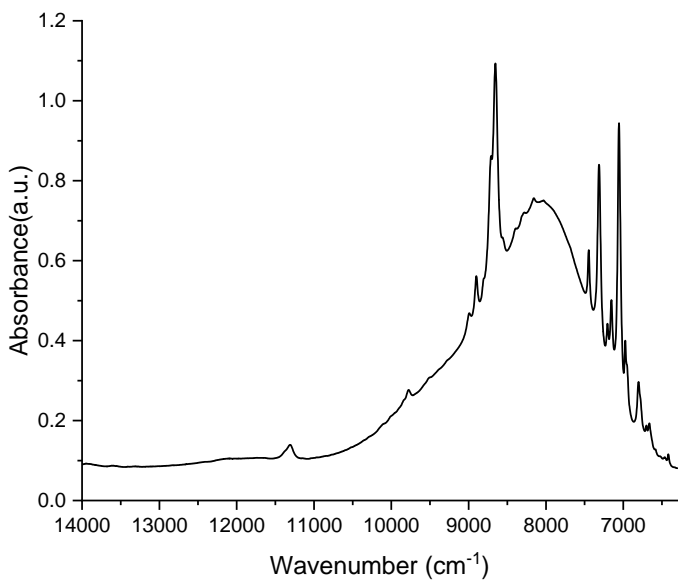


Figure S3. NIR spectrum of $[\text{Pt}(\text{L})\text{Py}]\text{[BF}_4]$ ($c = 0.1 \text{ mM}$) in CH_2Cl_2 at 298 K, $l = 1 \text{ cm}$.

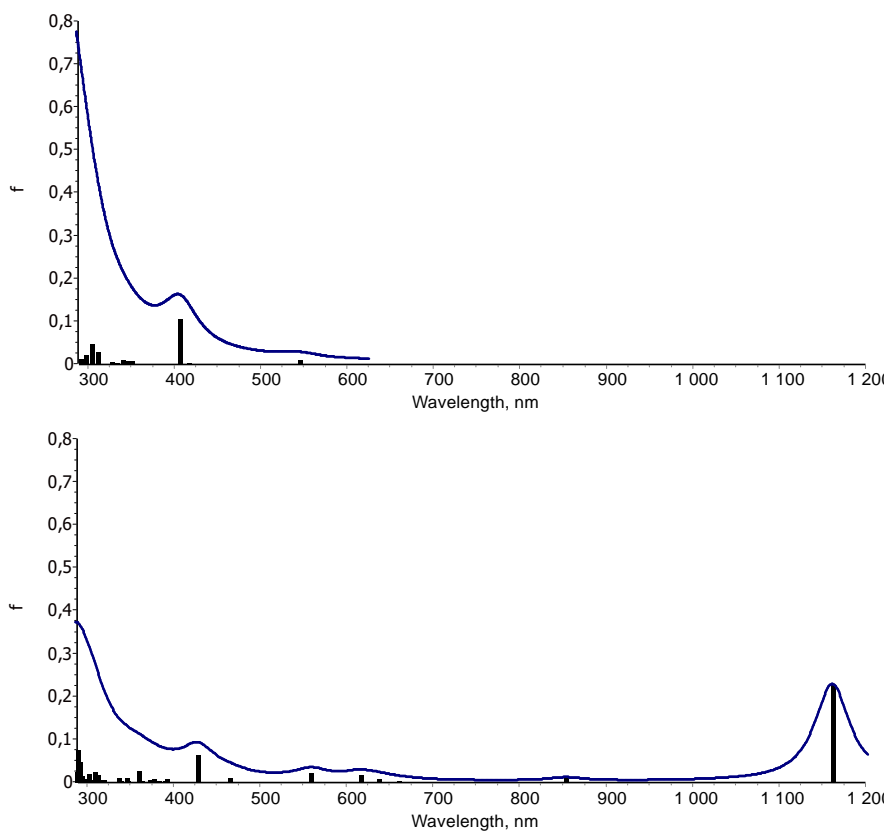
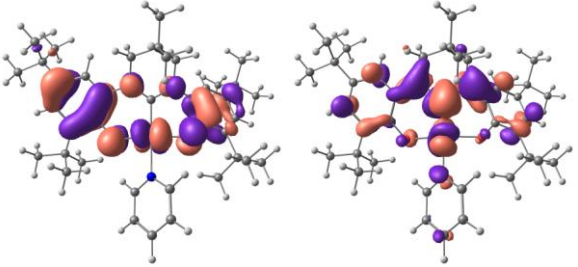
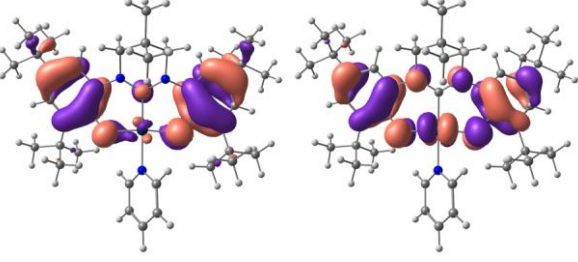
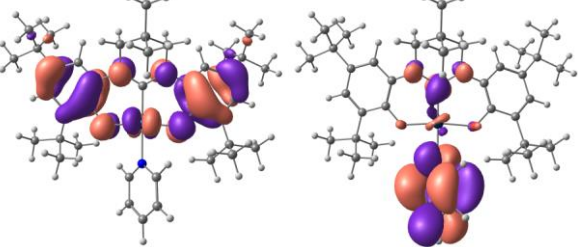
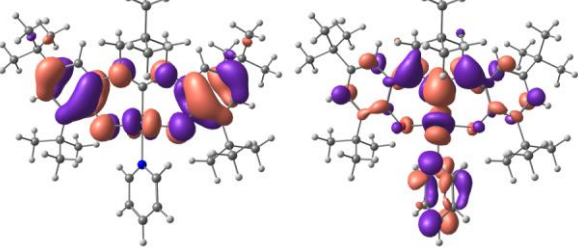


Figure S4. The calculated absorption spectra for $\text{Pt}(\text{L})\text{Py}$ (top graph) and $[\text{Pt}(\text{L})\text{Py}]\text{[BF}_4]$ (bottom graph). The vertical lines showing the position of electronic transitions and their intensity (f – oscillator strength) were broadened by the Lorentz function ($f.w.h.m. = 50 \text{ nm}$).

Table S1. Selected TD-DFT-calculated excitation energies (absorption wavelengths), oscillator strengths, and main compositions of the most important electronic transitions for $\text{Pt}(\text{L})\text{Py}$ and $[\text{Pt}(\text{L})\text{Py}]\text{[BF}_4]$.

λ	f	Transition
Pt(L)Py		
407	0.10	 <p>HOMO → LUMO+2 (95%, contour value = 0.03)</p>
[Pt(L)Py][BF₄]		
1162	0.23	 <p>β: HOMO → LUMO (97%, contour value = 0.03)</p>
429	0.06	 <p>α: HOMO → LUMO (58%, contour value = 0.03)</p>  <p>α: HOMO → LUMO+1 (32%, contour value = 0.03)</p>

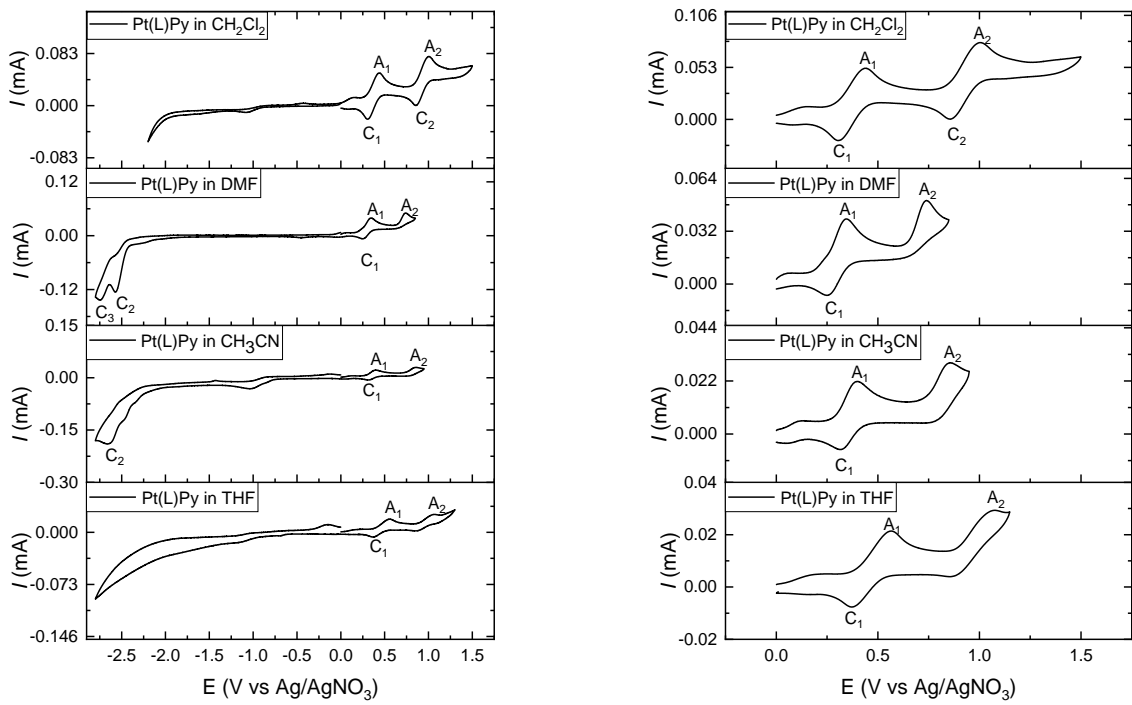


Figure S5. CV-curves recorded from a solution containing complex **Pt(L)Py** in different solvents ($c = 5$ mM) in the presence of $(n\text{-Bu}_4\text{N})\text{BF}_4$ (0.1 M) at the scan rate of $100 \text{ mV}\cdot\text{s}^{-1}$ on the GC working electrode ($T = 298 \text{ K}$).

Table S2. Peak potentials* on the CV-curves of complex **Pt(L)Py** obtained in different solvents.

Solvent	Cathodic peaks	$E_p^{\text{red}}, \text{V}$	Anodic peaks	$E_p^{\text{ox}}, \text{V}$
CH_2Cl_2	C_1	+0.85	A_1	+0.44
	C_2	+0.30	A_2	+1.01
DMF	C_1	+0.24	A_1	+0.34
	C_2	-2.57	A_2	+0.73
	C_3	-2.74		
CH_3CN	C_1	+0.32	A_1	+0.40
	C_2	-2.65	A_2	+0.85
THF	C_1	+0.36	A_1	+0.55
			A_2	+1.07

* The mentioned potentials are referred to the Ag/AgNO_3 .

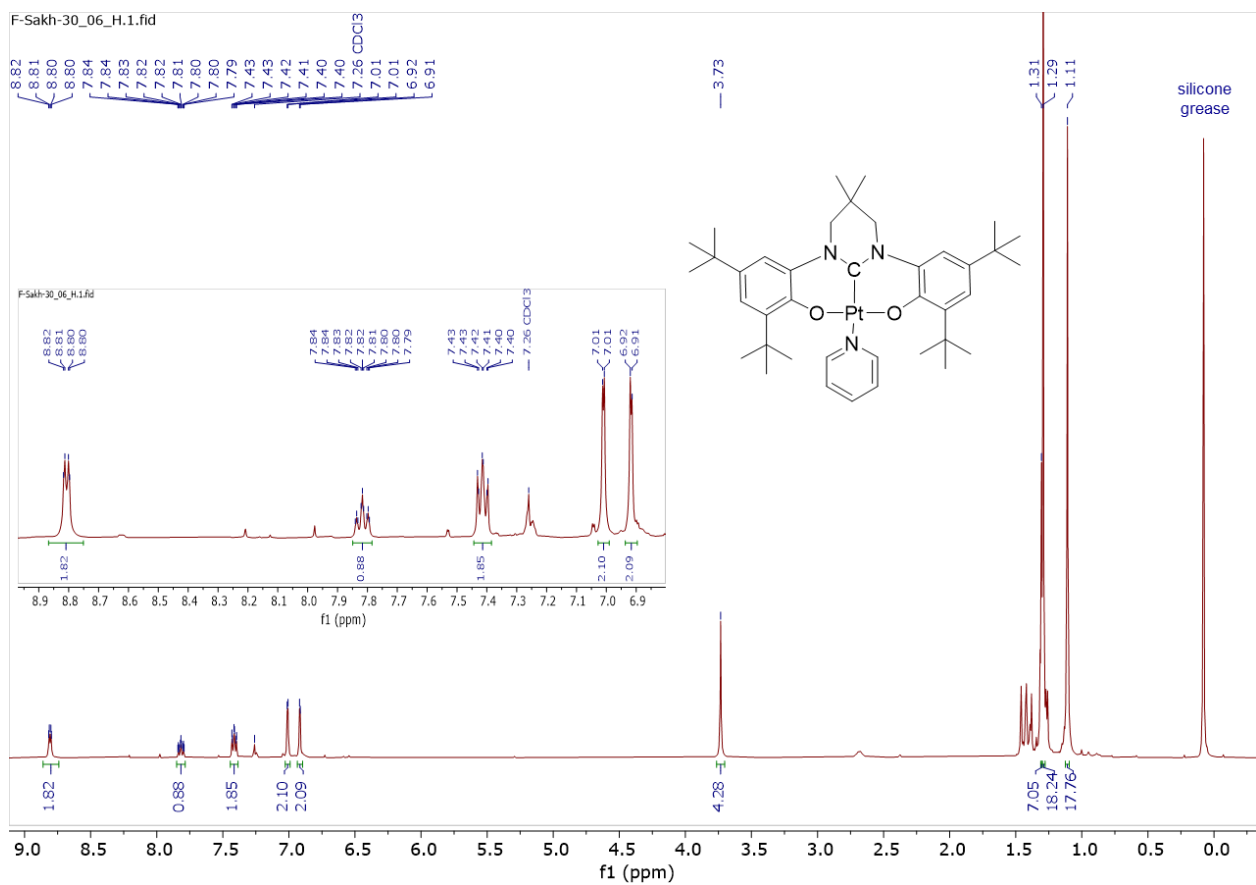


Figure S6. ^1H NMR (CDCl_3 , 400.17 MHz, 300 K) spectrum of Pt(L)Py.

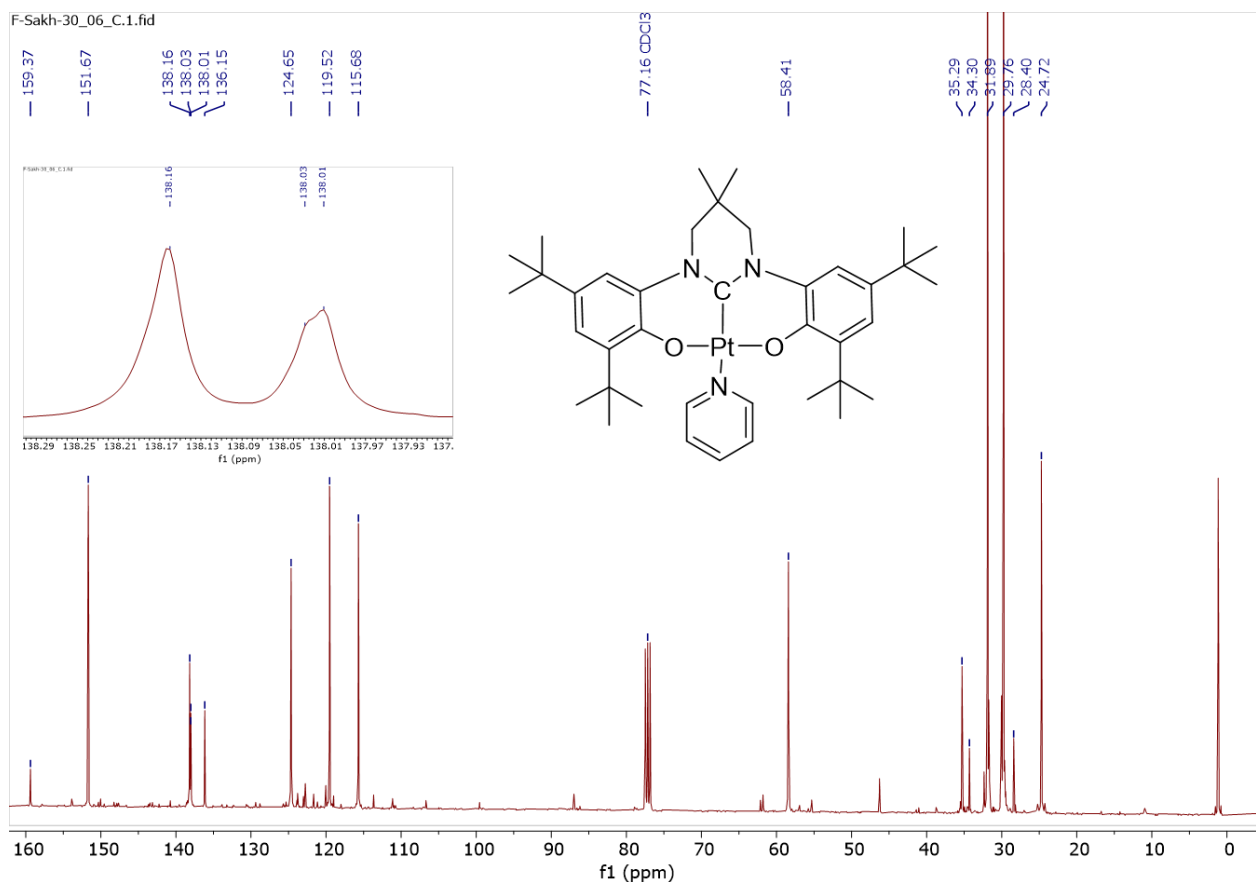


Figure S7. $^{13}\text{C}\{\text{H}\}$ NMR (100.62 MHz, CDCl_3 , 300 K) spectrum of Pt(L)Py.